Origin, criterion, and mechanism of vortex-core reversals in soft magnetic nanodisks under perpendicular bias fields

Myoung-Woo Yoo, Ki-Suk Lee, Dae-Eun Jeong, and Sang-Koog Kim[*]

Research Center for Spin Dynamics & Spin-Wave Devices, Nanospinics Laboratory, Research Institute of Advanced Materials,
Department of Materials Science and Engineering, Seoul National University, Seoul 151-744, Republic of Korea
(Received 14 September 2010; published 24 November 2010)

We studied dynamics of vortex-core reversals driven by circular rotating fields along with *static perpendicular magnetic fields* of different direction and strength. We found that the application of perpendicular fields H_p modifies the starting ground state of vortex magnetizations, thereby instigating the development of a magnetization dip $m_{z,dip}$ in the vicinity of the original core up to its threshold value, $m_{z,dip}^{cri} \sim -p$, which is necessary for vortex-core reversals, where p is the initial core polarization. We found the relationship of the dynamic evolutions of the $m_{z,dip}$ and the out-of-plane gyrofields h_z, which was induced, in this case, by vortex-core motion of velocity v, thereby their critical value relation $v_{cri} \propto h_z^{cri}$. The simulation results indicated that the variation of the critical core velocity v_{cri} with H_p can be expressed explicitly as $v_{cri}/v_{cri}^0 = (\rho/\rho_0)|-p-m_{z,dip}^g|$, with the core size ρ and the starting ground-state magnetization dip $m_{z,dip}^g$ variable with H_p, and for the values of v_{cri}^0 and ρ_0 at $H_p=0$. This work offers deeper and/or new insights into the origin, criterion and mechanism of vortex-core reversals under application of static perpendicular bias fields.

PACS number(s): 75.40.Gb, 75.40.Mg, 75.60.Jk

Vortex magnetization configurations[1–4] are of growing interest owing to their potential applications to nonvolatile information storage[5–9] and nano-oscillator devices,[10–12] not to mention the fundamental interest in their nontrivial dynamic characteristics including vortex-core reversals[13–19] and its gyrotropic mode.[20–23] It is well known that vortex-core reversals in ferromagnetic dots occur via the specific serial dynamic processes of the nucleation and annihilation of a vortex-antivortex (VAV) pair.[13,15,17–19] Recently, Lee *et al.*[24] found that the so-named critical velocity v_{cri} of the vortex-core motion is required for switching events. In fact, v_{cri} is independent not only of the driving forces typical of oscillating in-plane fields, rotating fields or currents, but also of their parameters and dot dimensions, while more generally, critical exchange energy has been considered as a criterion for VAV-mediated core reversals.[25] The measurable v_{cri} quantity has been experimentally measured,[26] and has been found to be expressed explicitly, on the basis of micromagnetic simulation results, as $v_{cri} = \eta \gamma A_{ex}^{1/2}$, with the proportional constant $\eta = 1.66 \pm 0.18$, the gyromagnetic ratio $\gamma = 2\pi \times 2.8$ MHz/Oe, and the exchange stiffness A_{ex}.[24] Inserting the numerical value of A_{ex} for a given material, v_{cri} is readily determined (e.g., for Permalloy (Py; $Ni_{80}Fe_{20}$), 330 m/s). Moreover, in cases where any driving forces are tuned to the eigenfrequency of a vortex in a given dot, the threshold field strength and current density are sufficiently small, since the vortex-core velocity can reach v_{cri} through the resonant gyrotropic motion.[7] v_{cri} thus is considered from the technical application point of view to be a useful quantity for the prediction of vortex-core reversal events and the determination of efficient driving force parameters such as frequency and strength.

Contrarily, Khvalkovskiy *et al.*[27] quite recently reported that v_{cri} can vary with the direction and strength of static fields H_p applied perpendicularly to the dot plane. Still other scenarios for a vortex-core reversal event have been found for some specific cases. For example, Kravchuk *et al.*[28] re-

ported that nucleation of a VAV pair is possible for a subsequent vortex-core switching event in the case of an immobile vortex core, which physical origin they ascribed to softening of the dipole magnon mode.[29] Also, Gliga *et al.*[25] reported possible vortex-core switching by application of spatially localized pulse fields in proximity to the vortex core; they found in this case that the vortex-core velocity is not necessary to reach v_{cri}. Therefore, not only does the physical origin of the variation of v_{cri} with H_p remain to be unraveled, but also the origin, criterion and mechanism of the relevant vortex-core reversals.

In this paper, we present dynamics of vortex-core reversals driven by circular rotating fields along with the application of static perpendicular magnetic fields, and reveal the physical origin of the variation in v_{cri} with H_p, as elucidated by micromagnetic simulations combined with quantitative interpretation. We calculated an out-of-plane gyrofield h_z that is produced by the deformation of vortex-core magnetizations induced by vortex-core motion,[14,30] and we revealed how it builds up a magnetization dip $m_{z,dip}$ near the original vortex core, until the critical value necessary for vortex-core reversal events is achieved. We found the correlations of the critical values and dynamic evolutions of $m_{z,dip}$, h_z and v, and discovered that the modification of the initial ground state of a vortex structure by H_p gives rise to the H_p dependences of h_z^{cri} and v_{cri}.

We chose micromagnetic simulation as our approach to this investigation, because it is a well-established, optimized tool for the study of magnetization dynamics on scales of a few nanometers spatially and ~ 10 ps temporally. For the simulations, we employed the OOMMF code[31] that incorporates the Landau-Lifshitz-Gilbert (LLG) equation[32] of motion of magnetization $\mathbf{M}$: $\partial \mathbf{M}/\partial t = -\gamma \mathbf{M} \times \mathbf{H}_{eff} + (\alpha/M_s)\mathbf{M} \times \partial \mathbf{M}/\partial t$, where $\mathbf{H}_{eff}$ is the total effective field, which in the present case includes, the demagnetizing, exchange and external static perpendicular fields, and additionally rotating field as a driving force of vortex excitations. We used a Py
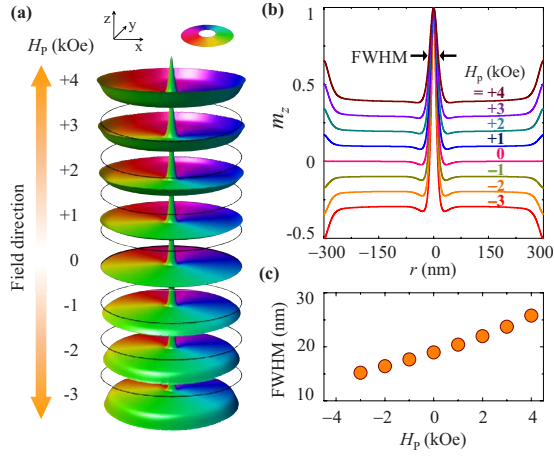
FIG. 1. (Color online) (a) Local magnetization distributions of initial static ground state under perpendicular magnetic fields of indicated field strengths H_p. The colors indicate local in-plane curling magnetizations (here in the counterclockwise rotation) as noted by the color wheel and the height of the surface corresponds to $m_z = M_z/M_s$. The spikes represent the upward cores. The black circles indicate the baseline corresponding to $m_z = 0$. (b) H_p-dependent m_z profiles from one edge to other edge, crossing core center. (c) H_p dependence of FWHM of the m_z profiles of cores.

nanodisk of radius $R = 300$ nm and thickness $L = 30$ nm. Uniform static fields were applied perpendicularly to the disk plane, the strength of which fields varied from $H_p = -3$ kOe to $+4$ kOe at an interval of 1 kOe.[33] The positive (negative) sign corresponds to the parallel (antiparallel) orientation of the vortex-core magnetization (polarization p) in the field direction [Fig. 1(a)]. We chose, as the driving force, the counterclockwise circular rotating field $\mathbf{H}_{\mathrm{CCW}} = H_0[\cos(\omega_H t)\hat{x} + \sin(\omega_H t)\hat{y}]$ because its application at rotating angular frequency ω_H tuned to the angular eigenfrequency ω_0 is the most effective means of vortex-polarization selective resonant excitations of, in this case, only the upward core, as demonstrated in earlier theoretical, experimental and simulation studies.[7,34,35] Because ω_0 changes with H_p as well, ω_H was varied as well.[36] The value of $H_0 = 20$ Oe, being larger than the threshold fields for all of the cases of H_p, was used to achieve the vortex-core reversals. The typical Py material parameters were used as follows: saturation magnetization $M_s = 8.6 \times 10^5$ A/m and exchange stiffness $A_{\mathrm{ex}} = 1.3 \times 10^{-11}$ J/m with zero magnetocrystalline anisotropy. The size of each individual cell was $2 \times 2 \times 30$ nm^3, and the Gilbert damping constant was $\alpha = 0.01$.

First we examined how application of different values of H_p and with opposite directions changes the initial ground state of the vortex structure, as reported earlier.[37] Such ground-state variation would be expected to be essential to vortex-core reversal dynamics. As can be seen from the perspective images of local magnetizations' spatial distribution in Fig. 1(a), there were distinct changes in the ground state. The H_p dependence of the m_z ($= M_z/M_s$) profile on the radial axis crossing the core center [Fig. 1(b)] reveals clearly that the in-plane magnetizations in the ground state are remar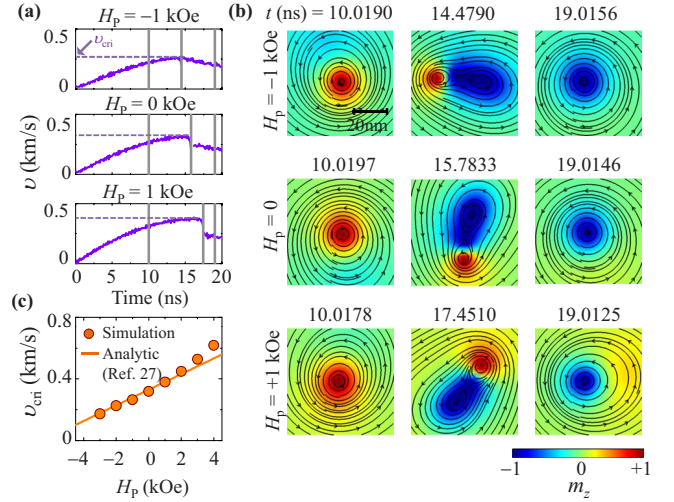kably deviated from the in-plane at the edge and the intermediate area around the core due to the Zeeman energy term of the perpendicular field. The modification of the m_z component at the very core center was negligible; the initial core magnetization $m_z = +1$ is maintained, due predominantly to the strong exchange coupling at the center, until much stronger perpendicular fields were applied.[38] Outwards from the core center, the Zeeman contribution became dominant, beginning to modify the m_z profile around the core, specifically (1) the m_z component level of the magnetization dip, $m_{z,\mathrm{dip}}$ (in the opposite direction with respect to the core magnetization), just outside the core and (2) the variation in the core size, represented by the full width at half maximum (FWHM) of the core m_z component [Figs. 1(b) and 1(c)]. With increasing negative H_p, the magnetization dip became deeper and the FWHM, smaller. These results are in good agreement with other reports.[27]

Next, in order to clarify how the above-mentioned ground-state modification by H_p affects vortex-core reversals, we plotted, as shown in Fig. 2(a), the vortex-core velocity before and after the core reversal events initiated by application of the field $\mathbf{H}_{\mathrm{CCW}}$. The instantaneous core velocity v was estimated from the trajectories of the vortex-core motions. Prior to the core reversals, the velocity increased, finally reaching its threshold value, v_{cri}. Then, the deformation of the entire magnetization structure of the vortex core was maximized and, which was accompanied by the serial processes of the nucleation of a newly formed VAV pair having the magnetization direction ($p = -1$) opposite to the original magnetization orientation ($p = +1$), and of the annihilation of the newly formed antivortex and the original

FIG. 2. (Color online) (a) Instantaneous velocity v of vortex-core motions versus time for different H_p values, examples here, $H_p = -1$, 0, and $+1$ kOe. The horizontal dashed lines represent the critical velocity, v_{cri}. (b) Snapshot plane-view images of spatial distribution of local magnetizations just before and after vortex-core reversal events, as well as at moment of formation of vortex and antivortex pair near original core. In those images, the colors of the surface correspond to the local m_z and the streamlines with the small arrows indicate the in-plane magnetization orientations. (c) H_p dependence of v_{cri} (closed circles) compared with result of explicit expression (solid line) $v_{\mathrm{cri}}(H_p) = v_{\mathrm{cri}}(0)(1 - H_p/H_c)$ reported in Ref. 27.
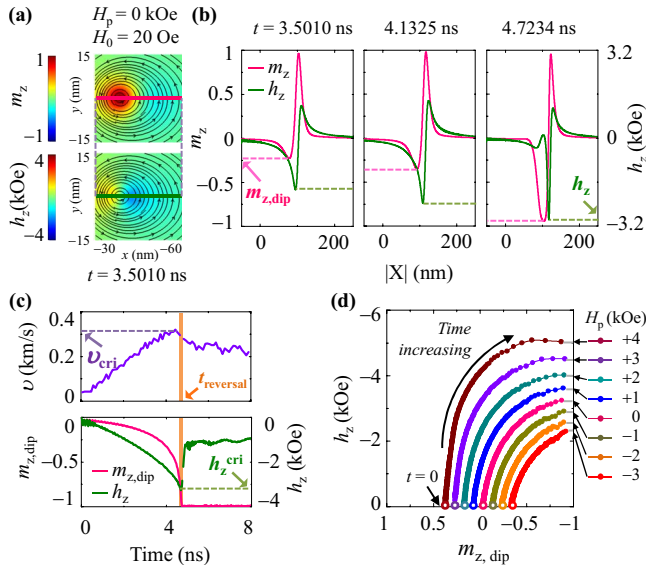
FIG. 3. (Color online) (a) Snapshot plane-view image for local distributions of m_z and h_z at selected moment ($t=3.501$ ns) just prior to vortex-core switching. (b) Profiles of m_z (red line) and h_z (green line) crossing vortex core. The value of $m_{z,\text{dip}}$ indicates the minimum value of the magnetization at the dip near the vortex core and h_z stands for the maximum magnitude of the local gyrofields at this moment. (c) Variations in v, h_z, and $m_{z,\text{dip}}$ with time, as well as relations of v_{cri}, h_z^{cri}, and $m_{z,\text{dip}}^{\text{cri}}$. (d) Relation of evolutions of h_z and $m_{z,\text{dip}}$ for different H_p values.

vortex,[13,15,17–19] for complete vortex-core reversals, as seen in Fig. 2(b). From the three H_p cases, the core reversal mechanism was the same as that in the known VAV-pair-mediated reversals; the only difference was the remarkable change in v_{cri} with H_p. In Fig. 2(c), the resultant H_p dependence of v_{cri} is plotted, showing an almost linear dependence on H_p over a wide but limited range. The simulation result is in good agreement with the explicit expression (solid line) of $v_{\text{cri}}(H_p)=v_{\text{cri}}^0(1-H_p/H_c)$ (Ref. 27) in the negative field region with a static perpendicular field $H_c\sim-6.5$ kOe, although there are some discrepancies in the positive field region. The value of $H_c\sim-6.5$ kOe, which was obtained from simulations on our dot dimensions, is the threshold strength required for core reversals only using the static perpendicular field. The v_{cri} variation with H_p is surprising, in that, for a given material and cases under $H_p=0$, v_{cri} is known to be independent of dot geometry and dimensions as well as type of the driving forces and their variable parameters.[15,24]

To elucidate the underling physics of such changes, we employ the dynamic evolution of gyrofields induced by the deformation of the magnetizations of the entire vortex structure due to vortex-core motion. The out-of-plane gyrofield is expressed as $h_z=-(1/\gamma M_s^2)(\mathbf{M}\times d\mathbf{M}/dt)_z$, as derived from the time-derivative term of the LLG equation.[14,39] From the numerical data of micromagnetic simulations, one can directly calculate the spatial distribution of the local h_z values as a function of time during vortex-core motion and even after the core's reversal event is complete. Figure 3(a) provides snapshot plane-view images of both the local h_z and m_z, taken at $t=3.501$ ns prior to the reversal. The m_z and h_z are strongly concentrated locally near the original vortex

core. The maximum of $|h_z|$ is found at about 6 nm away from the core center (the maximum of $|m_z|$). The serial profiles of the m_z and h_z shown in Fig. 3(b) show how the highly concentrated h_z influences the formation and consequent development of the indicated magnetization dip, $m_{z,\text{dip}}$ in the direction opposite to the original core magnetization (in this case $p=+1$).[14,30] As the $|h_z|$ grew larger, the $|m_{z,\text{dip}}|$ did likewise, finally reaching the critical value $m_{z,\text{dip}}^{\text{cri}}\sim-p$ for the initial polarization, here $p=+1$. As seen in the m_z profile of the magnetization dip, the width was larger than the original core width. The dip width included a newly formed antivortex as well, reflecting the fact that, when a new vortex is formed near the original vortex, the energetically stable structure is the vortex-antivortex-vortex configuration.[40]

Figure 3(c) shows the distinct time evolution of h_z, $m_{z,\text{dip}}$ with v. As v becomes faster, h_z grows more negative, making $m_{z,\text{dip}}$ further deepen, as explained above. When $m_{z,\text{dip}}$ reaches the threshold value $m_{z,\text{dip}}^{\text{cri}}\sim-p$, vortex-core reversals occur via the known mechanism, as depicted in Fig. 2(b). The critical value h_z^{cri} is achieved when $m_{z,\text{dip}}^{\text{cri}}\sim-p$, and at the same time, v_{cri} also is found because h_z is induced by vortex-core motion, and thus via $h_z\propto v$, as explained in Ref. 30. Next, in order to find the concrete correlation of the dynamic evolution of h_z and the development of $m_{z,\text{dip}}$, we plotted the variation in the temporal evolution of $m_{z,\text{dip}}$ with h_z for different H_p values, in Fig. 3(d). With increasing time, increases in h_z means increasingly negative values of $m_{z,\text{dip}}$, until the critical value $m_{z,\text{dip}}^{\text{cri}}\sim-p$. From the results, it was confirmed that the critical value h_z^{cri} is reached when $m_{z,\text{dip}}^{\text{cri}}\sim-p$, regardless of the values of H_p applied. Thus, more generally, $m_{z,\text{dip}}^{\text{cri}}\sim-p$ is the criterion for vortex-core reversal switching. As seen in Fig. 1, the applications of H_p modify the initial ground state of the magnetization dip, $m_{z,\text{dip}}^g$. With increasingly negative H_p, the value of $m_{z,\text{dip}}^g$ is already close to $-p$. $m_{z,\text{dip}}^g$ is a function of H_p, and as its value grows more negative, h_z^{cri} becomes smaller in order to reach $m_{z,\text{dip}}^{\text{cri}}\sim-p$. Thus $\Delta m_z(H_p)\sim m_{z,\text{dip}}^{\text{cri}}-m_{z,\text{dip}}^g(H_p)$ is the crucial factor in the determination of h_z^{cri} as a function of H_p.

In Fig. 4(a), we plotted the dependences of h_z^{cri} and v_{cri} on H_p. The decrease in v_{cri} with decreasing H_p is associated with the reduction in h_z^{cri}: h_z^{cri} is smaller, and so v_{cri} also is smaller, according to the relation of $v_{\text{cri}}\propto h_z^{\text{cri}}$, reported in our earlier work.[30] As mentioned above, the decrease of h_z^{cri} is related to the reduction of $\Delta m_z(H_p)\sim-p-m_{z,\text{dip}}^g(H_p)$ as well. The applications of H_p modify not only $m_{z,\text{dip}}$ but also the core size, denoted as $\rho=$FWHM. The variation of $\rho(H_p)\Delta m_z(H_p)$ plotted in Fig. 4(a) revealed mutual linear relationships between $v_{\text{cri}}(H_p)$, $h_z^{\text{cri}}(H_p)$, and $\rho(H_p)\Delta m_z(H_p)$. Further, the simulation results showed the correlations of $v_{\text{cri}}(H_p)\propto h_z^{\text{cri}}(H_p)$ and $h_z^{\text{cri}}(H_p)\propto\Delta m_z(H_p)\rho(H_p)$, along with the result, $v_{\text{cri}}(H_p)\propto\rho(H_p)\Delta m_z(H_p)$, as shown in Fig. 4(b). Finally we found the universal relation for any H_p

$$\frac{v_{\text{cri}}(H_p)}{\rho(H_p)|\Delta m_z(H_p)|}=\frac{v_{\text{cri}}^0}{\rho_0|\Delta m_z^0|}. \quad (1)$$

From Eq. (1), we obtained the following equation for $|\Delta m_z^0|=1$:

$$v_{\text{cri}}(H_p)=(v_{\text{cri}}^0/\rho_0)\rho(H_p)|\Delta m_z(H_p)|. \quad (2)$$

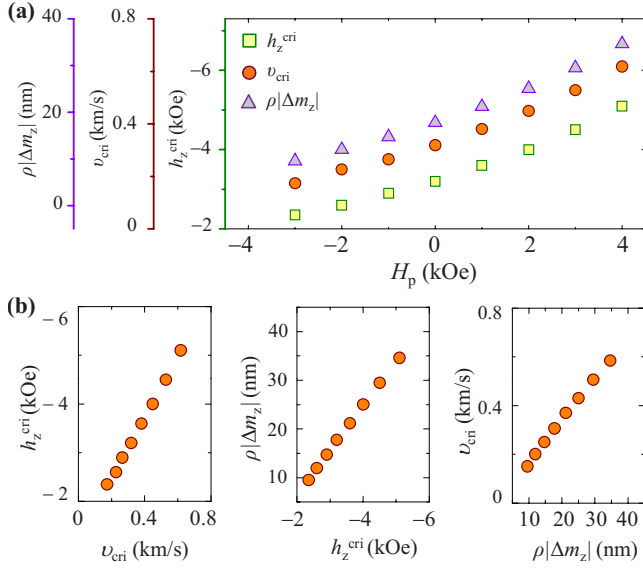FIG. 4. (Color online) (a) H_p dependence of h_z^{cri}, v_{cri}, and $\rho|\Delta m_z|$. (b) Linear relations of $h_z(H_p) \propto v_{cri}(H_p)$, $h_z(H_p) \propto \rho(H_p)\Delta m_z(H_p)$, and $v_{cri}(H_p) \propto \rho(H_p)\Delta m_z(H_p)$.

We next plotted v_{cri} versus H_p, as obtained from the simulations of vortex-core reversals under H_p for different dimensions, in Fig. 5. Surprisingly, the results (closed symbols) agreed well with the explicit expression (solid line) of Eq. (2), where $v_{cri}^0 = (1.66 \pm 0.18)\gamma A_{ex}^{1/2}$ and ρ_0 are the critical velocity and FWHM of the core, respectively, at $H_p = 0$. The analytical form predicts well the dynamic quantity v_{cri} as a function of H_p even in both negative and positive field regions, informing us that v_{cri} can be predicted simply with the values of v_{cri}^0 and ρ_0 for $H_p = 0$ from the magnetization profiles in the static ground state for different H_p values, $\rho(H_p)$ and $m_{z,dip}^g(H_p)$, without conducting further micromagnetic simulations of vortex-core reversal dynamics under H_p. Interestingly, the values of v_{cri}^0 and H_p dependences of ρ/ρ_0 and $|\Delta m_z|$ are independent of the dot dimensions; thus the expression of $v_{cri}(H_p) = (v_{cri}^0/\rho_0)\rho(H_p)|\Delta m_z(H_p)|$ is not variable with the dot dimensions.

Finally, we should note that in our previous report, the critical velocity was found not to change with dot dimensions and driving force parameters.[24] This is the case where the ground state of a vortex is not affected initially by other factors and the reversal is assisted with the motion of a movable vortex core. In the case of the application of H_p, the initial magnetization dip varies with H_p, and so the critical velocity, because it modifies $m_{z,dip}$.

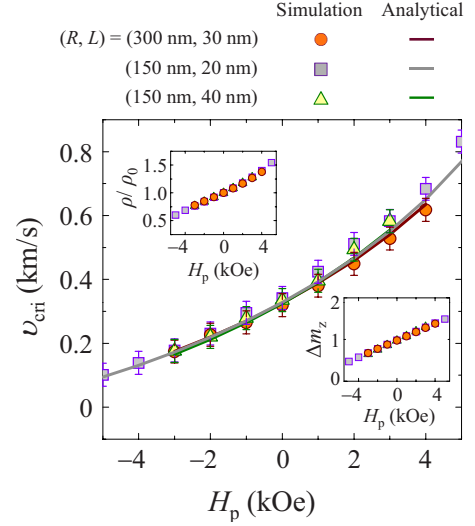In conclusion, we studied vortex-core reversal dynamics in ferromagnetic dots under static perpendicular magnetic

FIG. 5. (Color online) v_{cri} versus H_p, obtained from simulations (closed symbols) for indicated different dot dimensions, as compared with the results from analytical expression of $v_{cri} = (v_{cri}^0/\rho_0)\rho|\Delta m_z|$ (solid lines). For the different dimensions, the simulation results are within the error associated with the finite cell size employed for finding the vortex-core velocity. For all of the dimensions, the variations in $|\Delta m_z|$ and ρ/ρ_0 with H_p reflect the same trend, as shown in the insets.

fields, by micromagnetic simulations. It was found that the modification of the ground state of the vortex structure by H_p gives rise to variations in h_z^{cri} as well as v_{cri} with H_p. The results provide clear correlations of the dynamic evolution of v, h_z and $m_{z,dip}$ for the relevant core reversals. The critical values v_{cri} and h_z^{cri} are attained when $m_{z,dip}$ reaches the critical value, $m_{z,dip}^{cri} \sim -p$. The initial value of $m_{z,dip}$ in the ground state, which can be modified by H_p, determines those critical values of v_{cri} and h_z^{cri} for different H_p. The threshold value $m_{z,dip}^{cri} \sim -p$ is the criterion for VAV-pair-mediated core reversals. The previously found criterion, v_{cri}, is the criterion only where the VAV-mediated vortex-core reversals occur as assisted by vortex-core motion and where the initial ground state does not vary. We also found the concrete relations of $v_{cri} \propto h_z^{cri}$ and $h_z^{cri} \propto \rho\Delta m_z$ over a wide range of H_p, as well as $v_{cri}/v_{cri}^0 = (\rho/\rho_0)|\Delta m_z|$. This work offers, in the form of the results here presented, deeper insights into the fundamentals of vortex-core reversal dynamics.

*Author to whom correspondence should be addressed; sangkoog@snu.ac.kr

[1] A. Hubert and R. Schäfer, *Magnetic Domains* (Springer-Verlag, Berlin, 1998).

[2] J. Raabe, R. Pulwey, R. Sattler, T. Schweinbock, J. Zweck, and D. Weiss, J. Appl. Phys. **88**, 4437 (2000).

[3] T. Shinjo, T. Okuno, R. Hassdorf, K. Shigeto, and T. Ono, Science **289**, 930 (2000).

[4] A. Wachowiak, J. Wiebe, M. Bode, O. Pietzsch, M. Morgenstern, and R. Wiesendanger, Science **298**, 577 (2002).

[5] R. P. Cowburn, Nat. Mater. **6**, 255 (2007).

[6] J. Thomas, Nat. Nanotechnol. **2**, 206 (2007).

[7] S.-K. Kim, K.-S. Lee, Y.-S. Yu, and Y.-S. Choi, Appl. Phys. Lett. **92**, 022509 (2008); S.-K. Kim, K.-S. Lee, Y.-S. Choi, and Y.-S. Yu, IEEE Trans. Magn. **44**, 3071 (2008).

[8] S. Bohlens, B. Krüger, A. Drews, M. Bolte, G. Meier, and D. Pfannkuche, Appl. Phys. Lett. **93**, 142508 (2008).

[9] Y.-S. Choi, M.-W. Yoo, K.-S. Lee, Y.-S. Yu, H. Jung, and S.-K. Kim, Appl. Phys. Lett. **96**, 072507 (2010).

[10] S. I. Kiselev, J. C. Sankey, I. N. Krivorotov, N. C. Emley, R. J. Schoelkopf, R. A. Buhrman, and D. C. Ralph, Nature (London) **425**, 380 (2003).

[11] Q. Mistral, M. van Kampen, G. Hrkac, J.-V. Kim, T. Devolder, P. Crozat, C. Chappert, L. Lagae, and T. Schrefl, Phys. Rev. Lett. **100**, 257201 (2008).

[12] A. Dussaux, B. Georges, J. Grollier, V. Cros, A. V. Khvalkovskiy, A. Fukushima, M. Konoto, H. Kubota, K. Yakushiji, S. Yuasa, K. A. Zvezdin, K. Ando, and A. Fert, Nat. Commun. **1**, 8 (2010).

[13] B. Van Waeyenberge, A. Puzic, H. Stoll, K. W. Chou, T. Tyliszczak, R. Hertel, M. Fähnle, H. Brückl, K. Rott, G. Reiss, I. Neudecker, D. Weiss, C. H. Back, and G. Schütz, Nature (London) **444**, 461 (2006).

[14] K. Yamada, S. Kasai, Y. Nakatani, K. Kobayashi, H. Kohno, A. Thiaville, and T. Ono, Nat. Mater. **6**, 270 (2007).

[15] S.-K. Kim, Y.-S. Choi, and K.-S. Lee, Appl. Phys. Lett. **91**, 082506 (2007).

[16] S. Choi, K.-S. Lee, K. Yu. Guslienko, and S.-K. Kim, Phys. Rev. Lett. **98**, 087205 (2007).

[17] Q. F. Xiao, J. Rudge, E. Girgis, J. Kolthammer, B. C. Choi, Y. K. Hong, and G. W. Donohoe, J. Appl. Phys. **102**, 103904 (2007).

[18] R. Hertel, S. Gliga, M. Fähnle, and C. M. Schneider, Phys. Rev. Lett. **98**, 117201 (2007).

[19] K.-S. Lee, K. Yu. Guslienko, J.-Y. Lee, and S.-K. Kim, Phys. Rev. B **76**, 174410 (2007).

[20] B. E. Argyle, E. Terrenzio, and J. C. Slonczewski, Phys. Rev. Lett. **53**, 190 (1984).

[21] K. Yu. Guslienko, B. A. Ivanov, V. Novosad, H. Shima, Y. Otani, and K. Fukamichi, J. Appl. Phys. **91**, 8037 (2002).

[22] J. P. Park, P. Eames, D. M. Engebretson, J. Berezovsky, and P. A. Crowell, Phys. Rev. B **67**, 020403 (2003).

[23] S.-B. Choe, Y. Acremann, A. Scholl, A. Bauer, A. Doran, J. Stöhr, and H. A. Padmore, Science **304**, 420 (2004).

[24] K.-S. Lee, S.-K. Kim, Y.-S. Yu, Y.-S. Choi, K. Yu. Guslienko, H.-S. Jung, and P. Fischer, Phys. Rev. Lett. **101**, 267206 (2008).

[25] S. Gliga, Y. Liu, A. Kakay, and R. Hertel, 11th Joint Magnetism and Magnetic Materials-Intermag Conference, Washington DC, 2010, Oral GD-07 (unpublished).

[26] A. Vansteenkiste, K. W. Chou, M. Weigand, M. Curcic, V. Sackmann, H. Stoll, T. Tyliszczak, G. Woltersdorf, C. H. Back, G. Schütz, and B. VanWaeyenberge, Nat. Phys. **5**, 332 (2009).

[27] A. V. Khvalkovskiy, A. N. Slavin, J. Grollier, K. A. Zvezdin, and K. Yu. Guslienko, Appl. Phys. Lett. **96**, 022504 (2010).

[28] V. P. Kravchuk, Y. Gaididei, and D. D. Sheka, Phys. Rev. B **80**, 100405 (2009).

[29] Y. Gaididei, V. P. Kravchuk, D. D. Sheka, and F. G. Mertens, Phys. Rev. B **81**, 094431 (2010).

[30] K. Yu. Guslienko, Ki-Suk Lee, and Sang-Koog Kim, Phys. Rev. Lett. **100**, 027203 (2008).

[31] The version of the OOMMF code used is 1.2a4. See http://math.nist.gov/oommf

[32] L. D. Landau and E. M. Lifshitz, Phys. Z. Sowjetunion **8**, 153 (1935); T. L. Gilbert, Phys. Rev. **100**, 1243 (1955) [Abstract only; full report, Armor Research Foundation Project No. A059, Supplementary Report, May 1, 1956] (unpublished).

[33] Under fields smaller than -3 kOe, it is too difficult to observe the vortex-core dynamics because, in this system, they are very unstable. But under fields larger than 4 kOe, it is difficult to calculate the critical core velocity, because the threshold field for the vortex-core reversal is very high.

[34] K.-S. Lee and S.-K. Kim, Phys. Rev. B **78**, 014405 (2008).

[35] M. Curcic, B. Van Waeyenberge, A. Vansteenkiste, M. Weigand, V. Sackmann, H. Stoll, M. Fähnle, T. Tyliszczak, G. Woltersdorf, C. H. Back, and G. Schütz, Phys. Rev. Lett. **101**, 197204 (2008).

[36] From the simulations, we determined the variation in ω_0 with H_p(kOe), which occurs as follows: $\omega_0(-3)=2\pi\times290$ MHz, $\omega_0(-2)=2\pi\times340$ MHz, $\omega_0(-1)=2\pi\times380$MHz, $\omega_0(0)=2\pi\times430$ MHz, $\omega_0(+1)=2\pi\times470$ MHz, $\omega_0(+2)=2\pi\times520$ MHz, $\omega_0(+3)=2\pi\times560$ MHz, and $\omega_0(+4)=2\pi\times610$ MHz.

[37] B. A. Ivanov and G. M. Wysin, Phys. Rev. B **65**, 134434 (2002).

[38] T. Okuno, K. Shigeto, T. Ono, K. Mibu, and T. Shinjo, J. Magn. Magn. Mater. **240**, 1 (2002); A. Thiaville, J. M. García, R. Dittrich, J. Miltat, and T. Schrefl, Phys. Rev. B **67**, 094410 (2003).

[39] A. A. Thiele, Phys. Rev. Lett. **30**, 230 (1973).

[40] E. E. Huber, Jr., D. O. Smith, and J. B. Goodenough, J. Appl. Phys. **29**, 294 (1958); R. D. Gomez, T. Luu, A. Pak, K. Kirk, and J. Chapman, *ibid.* **85**, 6163 (1999).